

Experimental Investigation of the Velocity Field in Buoyant Diffusion Flames Using PIV and TPIV Algorithm

LULU SUN¹, XIANGYANG ZHOU¹, SHANKAR MAHALINGAM¹, and DAVID R. WEISE²

¹Department of Mechanical Engineering
University of California
Riverside, CA 92521

²Forest Fire Laboratory, Pacific Southwest Research Station
USDA Forest Service
²4955 Canyon Crest Drive
Riverside, CA

ABSTRACT

We investigated a simultaneous temporally and spatially resolved 2-D velocity field above a burning circular pan of alcohol using particle image velocimetry (PIV). The results obtained from PIV were used to assess a thermal particle image velocimetry (TPIV) algorithm previously developed to approximate the velocity field using the temperature field, simultaneously captured by an infrared (IR) thermal camera. By tracing “thermal particles,” which were assumed to be virtual particles that corresponded to pixels of temperature values in successive IR images, the TPIV algorithm estimated a larger scale instantaneous velocity field than either a single-point velocity measurement (e.g., LDV) or the area velocity measurement such as PIV. Instantaneous velocity fields obtained from both methods are presented. Time series vertical velocity profiles and time-averaged velocity vector fields are compared. The comparison demonstrates the applicability and performance of the TPIV algorithm in wildfire research.

KEYWORDS: PIV, velocity, temperature, IR

INTRODUCTION

Fire spread in wildland fuels is sustained by the combined effects of energy release due to fuel combustion, convective heat transfer, flame and ember radiation heat transfer, and energy transfer through mechanical advection effects such as rolling embers and spotting. Intense fire vortices on the scale of meters that promote convective heat transfer have been hypothesized to play a fundamental role in the physics of fire spread [1-3]. Fendell [4] presented an alternative hypothesis to vortices to describe unburned strips in large fires known as “crown streets.” McRae and Flannigan [5] describe fire vortices that in one case were observed to rip out and loft standing trees. Clarke et al. [6] observed a fire vortex rising more than 3 km above ground level with flaming materials that were visible from a distance of about 2 km. Therefore, fire vortices not only pose a hazard to nearby firefighters, but are potentially an important fire spread mechanism through both local fire dynamics and the ability to loft flaming objects into areas well removed from the original fire front. Although there is limited data existing to describe fire spread rate and some qualitative aspects of wildfire behavior, there is no data to reveal the small temporal and spatial scale involved in the convective processes that help determine fire spread [6].

Particle image velocimetry (PIV) technique has been widely used in non-reacting flows [7] and combustion environments to measure flow velocities [8-14] at laboratory scales. It provides a shorter acquisition time and increased measurement area compared to single-point measurement techniques such as Laser Doppler Velocimetry (LDV). An important aspect of PIV is its ability to measure the vorticity field and spatial correlations [15-16]. The utility of PIV is limited by factors such as the ability to seed particles of the right size in the flow, the limited image size, and the camera framing rate. These limitations potentially restrict the usefulness of PIV in wildfire field research.

Infrared (IR) thermal cameras have been used successfully to detect and map the temperature field within wildfires [6, 17-21]. With increasingly sensitive image converters and improvement of software, large scale, high resolution and high frequency IR images are available now and offer some useful advantages to fire researchers. An IR image represents a sheet of data in the x - z plane with the y (depth coordinate) varying over the image. It allows investigation of physical mechanisms involving fire spread rate through use of image flow analysis. We recently developed a thermal particle image velocity (TPIV) algorithm for nonintrusively estimating flow velocities within the vicinity of a flame through IR camera [22]. TPIV follows the method established in gradient-based algorithms [6], and uses the basic idea of the PIV technique. By tracing “thermal particles” across successive IR images, the TPIV algorithm can provide a larger scale instantaneous velocity measurement area than either a single-point velocity measurement [23-24] or the area velocity measurement such as PIV. In TPIV, the seed particles are represented by “thermal particles,” which are assumed as virtual particles that correspond to pixels of temperature values resolved in IR images. The signal from a “thermal particle” is the irradiance measured by an IR thermal camera. It is assumed that “thermal particles” rotate and translate behaving like fluid particles and their temperatures are conserved over the short time step between images that is required for analysis. For details of the technique, see Zhou et al. [22]. However, they did not directly validate the TPIV method, even though the results appeared promising.

The objective of this paper is to measure two-dimensional instantaneous velocity fields in flames above a cylindrical container filled with alcohol using the PIV technique. The results obtained from PIV were then used to assess the estimates of the velocity from IR images, simultaneously captured by an IR camera.

EXPERIMENTAL SETUP

Infrastructure

A schematic of the experimental setup is shown in Fig. 1. An aluminum fuel pan (diameter 88 mm, depth 53 mm) was placed in the middle of a 0.6 m \times 0.6 m \times 1 m enclosure to protect the flame from ambient air disturbances. Two of the lateral sides of the enclosure were aluminum sheets painted with hi-heat black paint to prevent laser light reflection. Tempered glass was installed on one side of the enclosure to receive the laser sheet. IR emission from the fire passed through a surface covered by polyethylene film for flame temperature detection by the IR camera. The top of the enclosure was connected to a fume hood so that the combustion products eventually discharged into the atmosphere. The hood was connected to an exhaust fan running at a low speed to keep the flame steady. The bottom of the enclosure was made of a hard metal screen to hold the fuel container and to permit seeded particles to pass through. In order to make the seed particles and fresh air entrain the flame as uniformly as possible, a fine aluminum

screen was placed at the bottom of the enclosure with a 20 cm gap between the bottom and the screen.

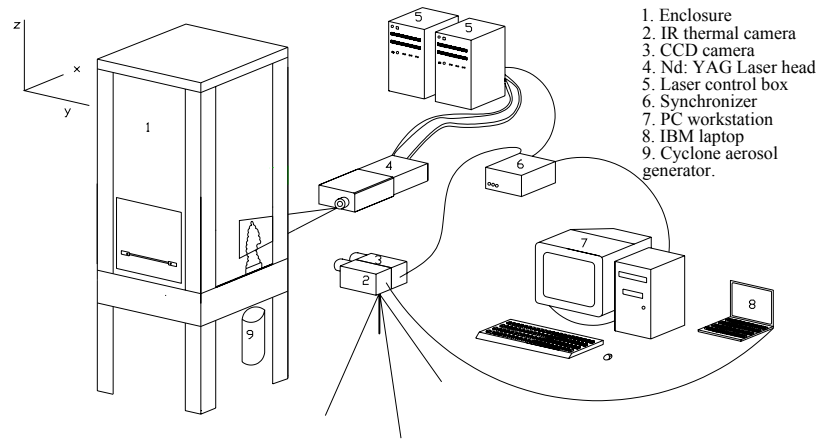


Fig. 1. Schematic of experimental setup.

PIV System

A double-pulsed Nd: YAG laser (Big Sky Laser Technologies, Inc, model CFR400) operating at a wavelength of 532 nm (230 mJ per pulse) and a pulse rate of 15 Hz was used in our PIV measurement. The laser beam was expanded into a 567 mm high by 0.212 mm thick sheet to illuminate the particles in the test section. The overlapped core beams were expanded into a 20-degree diverging light sheet using focusable sheet-forming optics, which includes a spherical lens (2000 mm focal length) and a cylindrical lens (15 mm focal length). A high resolution POWERVIEW 2M CCD camera (TSI Inc., 1660×1200 pixels array, 30 Hz with 12 bit digital output) with a 50 mm $f/1.8$ Nikkor lens recorded particle image pairs without image-order ambiguity allowing for the use of cross-correlation methods to determine velocity vectors. To reduce the luminosity of the flame, a bandpass filter (532 nm center, 1.5nm bandwidth) was placed in front of the camera lens. A LASERPULSE Synchronizer (TSI Inc.) triggered the laser pulse and the camera with correct sequences and timing through a 2.66 GHz dual-processor workstation (Intel® Xeon™). The time difference between laser pulses was 1000 μ s, yielding a maximum particle displacement of 25% of the square interrogation area length. INSIGHT™ 3.5 software package (TSI Inc.) was used to find the average velocity displacement in each interrogation area (32×32 pixels, 50% overlap) of the image by means of FFT-based cross-correlation algorithms. The data was collected in a 600 mm × 420 mm domain (or 1600×1192 pixels) and the images were processed to yield a velocity vector field of 99×73 pixels.

Al_2O_3 particles with nominal diameter of 1 μ m (Fig. 2a) were chosen as seed particles for their high refractive index and high melting point (≈ 2345 °K) [25]. Compressed air (outlet flow velocity = 0.05 m/s) was seeded with Al_2O_3 particles gathered from a cyclone aerosol generator and injected vertically upwards into the enclosure (Fig. 2b). The generator, which insured uniform distribution of particles, was based on the design by Glass et al. [26]. A compressed air line was attached to the bottom of this generator so that the particles could be continuously dispersed. The aerosol was drawn from the top of the generator.

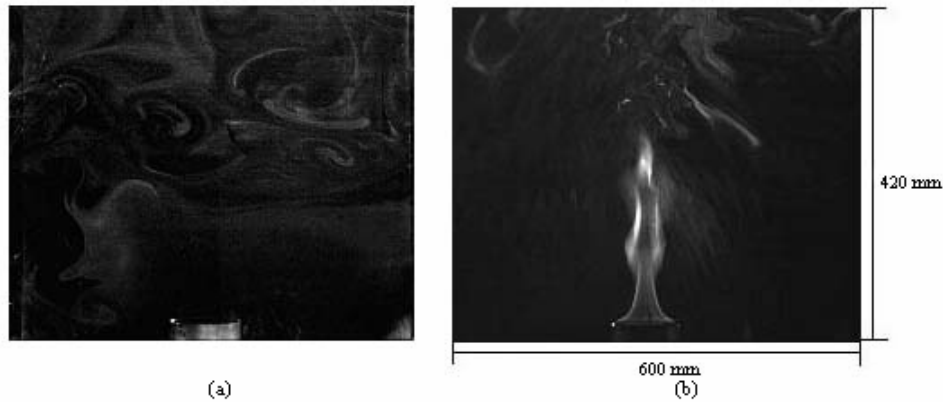


Fig. 2. Photographs of Al_2O_3 particles with (a) and without (b) alcohol flame illuminated by dual-pulse Nd: YAG laser. Figure 2b was acquired with a bandpass filter.

IR Camera System

Temperature images were captured by a FLIR ThermaCAM SC500 with an uncooled microbolometer 320×240 pixel focal plane array sensitive to the 7.5 to $13 \mu\text{m}$ spectral range. Temperature changes as small as $0.1 \text{ }^\circ\text{C}$ can be detected and the maximum frame rate 60 Hz was used in our experiments. An overall flame emissivity of 0.7 was used based on the temperature estimate measured by a 24 gauge (0.51 mm bead diameter) type K thermocouple above the fuel bed. ThermaCAM Researcher 2001 software (FLIR systems) was used to display and analyze instantaneous temperature images of the entire flame on a laptop computer. Three successive temperature images were then used as input for the TPIV algorithm to estimate the velocity field associated with the central image [22]; this resulted in an effective frame rate of 20 Hz for the calculated instantaneous velocity field. In our experiment, the TPIV algorithm utilized a patch size of 21×21 pixels on a sequence of temperature images to derive the velocity field.

Combination of the PIV and IR Systems

The PIV and IR systems were combined to obtain the coupled instantaneous velocity-temperature information. The digitized images captured from the CCD and IR cameras were transferred to computers for storage and post processing. One disadvantage of the current configuration is different capture planes from laser sheet and IR imagery. The laser sheet of PIV system was aligned vertically along the diameter of the fuel pan, while the IR imagery represented an average temperature over a significant depth into the flame front and corresponding derived velocity components are representative for similar depths (see Fig. 3). Due to flame symmetry, we assumed the derived-velocity field from TPIV algorithm had similar motions as that obtained from PIV system. This assumption was key to verification of the accuracy of the results of the TPIV algorithm which, in turn determined the potential application of the TPIV algorithm to wildland fire research. The base of the fuel container blocked seed particles from entering the flame zone resulting in a low density of seed particles close to the fuel surface, making velocity measurements in this region via PIV particularly difficult. Thus image analysis focused on the upper part of the flame. The image area extended from 100 mm to 400 mm downstream of the container mouth (Fig. 4). Figure 4a shows an example of infrared image of the temperature field of the alcohol fire captured by IR camera and the numbers denote

temperature values of contours in degrees Kelvin. Figure 4b shows an example of the instantaneous velocity field obtained from the PIV system at the same time. The black circle marks the location of measurement shown in Fig. 5 and Fig. 7. The outline of the fuel container is sketched at the bottom of Fig. 4b. Because PIV and IR data were acquired with different detectors, frame rates and resolution, suitable scaling, cropping and matching of the images were performed. The physical scale is determined from the ruler markers captured in the image. The matched image spans a 150 mm × 300 mm region of flame. As there was no external triggering option to synchronize the IR and PIV systems, the velocity field, which is measured by PIV at a rate of 15 Hz, and IR images recorded at 60 Hz frame rate cannot be recorded at the same time instances. We recorded PIV and IR images before starting the experiment and synchronized their first images by post processing the results separately.

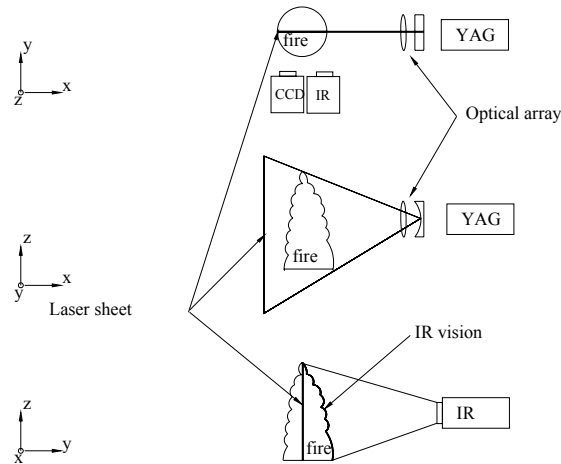


Fig. 3. Schematic view of the pool fire in the experiment.

Analysis of Combined Measurements

Data used for analysis was collected during the quasi-steady puffing state of the fire. Cetegen and Ahmed [27] summarized the puffing frequencies f in sec^{-1} , as a function of container diameter D in meters, of a fire and a good approximation can be written as

$$f \approx 1.5D^{-1/2} \quad (1)$$

Analysis of successive temperature data obtained from the IR camera suggested a puffing frequency of 6 Hz (see Fig. 5). The location of the temperature data is described as a black circle in Fig. 4. Three seconds of recording yielded 45 frame images from the CCD camera and 180 frame images from the IR camera providing sufficient data used for detailed analysis and calculation of time-averaged velocity fields. The instantaneous and time-averaged velocity fields obtained from PIV and the TPIV algorithm are presented in the next section. Two time series of vertical velocity at about mid flame height from PIV and the TPIV algorithm are compared.

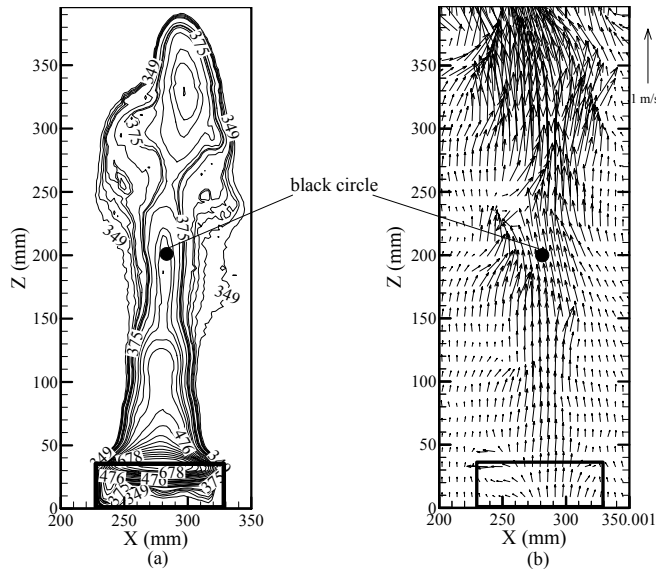


Fig. 4. Instantaneous temperature field captured from the IR camera (a), velocity vector image obtained from PIV system at the same time (b).

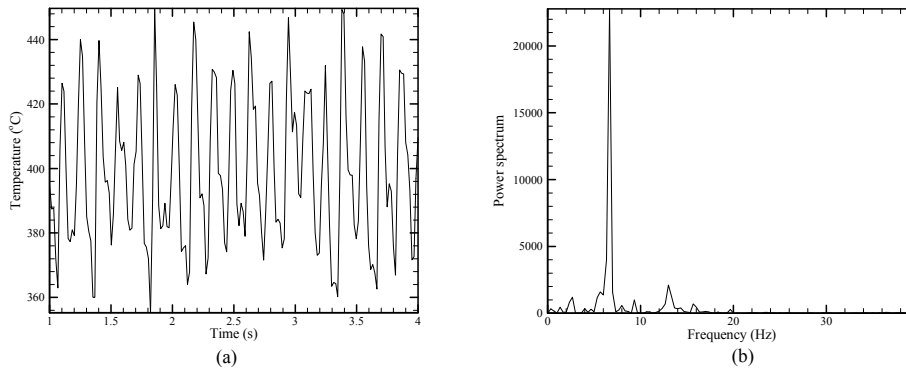


Fig. 5. Temperature time history (a), and corresponding frequency spectrum (b).

RESULTS AND DISCUSSION

Instantaneous Velocity Field

In column 1 and 2 of Fig. 6, we show successive velocity vector fields obtained from PIV and the TPIV algorithm respectively over one puff cycle, and in column 3 the temperature images captured by the IR camera corresponding to the velocity vector fields in column 2 are presented. The three rows represent three evenly spaced time slices during the puff cycle and the first row corresponds to the low value of the vertical velocity at ~ 1 s in Fig. 7. The second row occurs 0.07 s later and represents the velocity field at one third phase of the cycle. The last row occurs 0.07 s later, and represents the velocity field at two third phase of the cycle. The velocity fields in column 1 obtained from the PIV system are the original images processed from INSIGHT™ 3.5 software,

while the velocity fields in column 2 estimated from the TPIV algorithm are post processed images based on the IR temperature images in column 3. Clearly, the images obtained by both methods all show high acceleration and large vertical structures. However, because of the entrainment of cold air at the edge of the fire plume, the temperature is relatively uniform, and consequently, the velocity estimated by the TPIV algorithm in the non-flame region is inaccurate [22].

Time Series Vertical Velocity Data

For further detailed comparison, successive instantaneous velocity images obtained from both methods were converted into time series at the position of $x = 280$ mm and $y = 200$ mm. The measurement point is marked in Fig. 4b with a black circle, and the result is displayed in Fig. 7. The puff numbers noted in Fig. 7 correspond to the PIV data while the dashed line shows an extra puff found from the TPIV data. Even though the periods of the puff cycles vary slightly from cycle to cycle, on average, a cycle occurs every 0.2 s (5 puffs per second) based on PIV data, which is consistent with the empirical correlation (see Eq. 1 and [27]). However, the frequency (6 Hz) obtained from TPIV data is about 20% higher. Overall From Fig. 7, the vertical velocity data estimated from the TPIV algorithm and the PIV system show similar motion trends, but the data from TPIV algorithm gives higher fluctuation in amplitude than that obtained from the PIV system and the averaged vertical velocity from the TPIV algorithm is 0.75 m/s, which is a little lower than that from PIV system (0.81 m/s). These discrepancies may be attributable to several reasons. Even though the frame rate of velocities estimated by TPIV algorithm is 20 Hz which is comparable to 15 Hz from PIV calculation, each frame of the velocity field obtained from PIV was calculated based on laser pulses of 1000 μ s, which is far higher than the spacing between consecutive IR images (1/60 s) used to estimate velocities from TPIV algorithm. The relatively large time difference between consecutive images definitely will affect the accuracy of the velocity estimation from TPIV algorithm. Also the particle number density utilized in the PIV system cannot be controlled very well which also affects velocity calculation from PIV system. A more detailed analysis is clearly required.

Time-averaged Velocity Field

Figures 8a and 8b show a comparison of the time-averaged velocity vectors over 3 seconds obtained from the PIV system and that estimated from the TPIV algorithm. Figure 8c shows the corresponding time-averaged temperature contour obtained from the IR camera. A comparison with the instantaneous velocity fields in Fig. 6 shows that time averaging smears the vertical nature of the flow and yields a symmetric distribution in the observed region. Overall, the TPIV estimate is in reasonable agreement with the PIV. The peak vertical velocity calculated from the PIV system is 1.02 m/s, which is somewhat higher than 0.83 m/s estimated from the TPIV algorithm. Figure 9 shows radial profiles of time-averaged vertical velocity obtained from PIV and TPIV algorithm at the vertical height of 200 mm. Overall, the profiles appear to be Gaussian, but PIV data appears smoother than TPIV data. TPIV algorithm currently is only a basic version, there are no filters or other statistical methods used to improve results and based on the discussion in Zhou et al. [22], the low IR frame rate also affects the estimated velocity [28]. We do not expect that the TPIV algorithm will provide more accurate velocity estimates than PIV. We only want to demonstrate that the TPIV algorithm is a feasible tool to rapidly estimate velocities in a wildland fire.

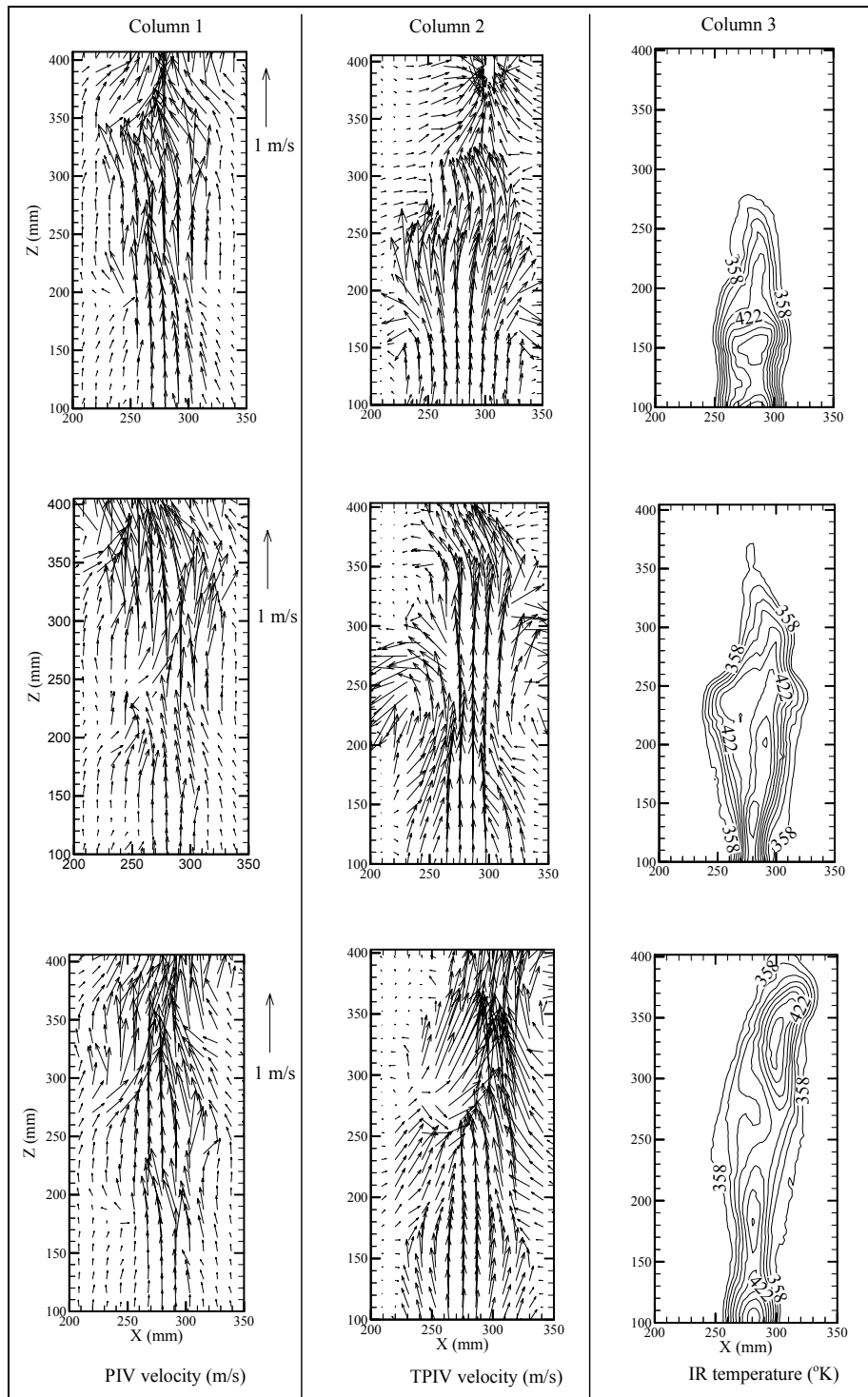


Fig. 6. Three phases of a puff cycle.

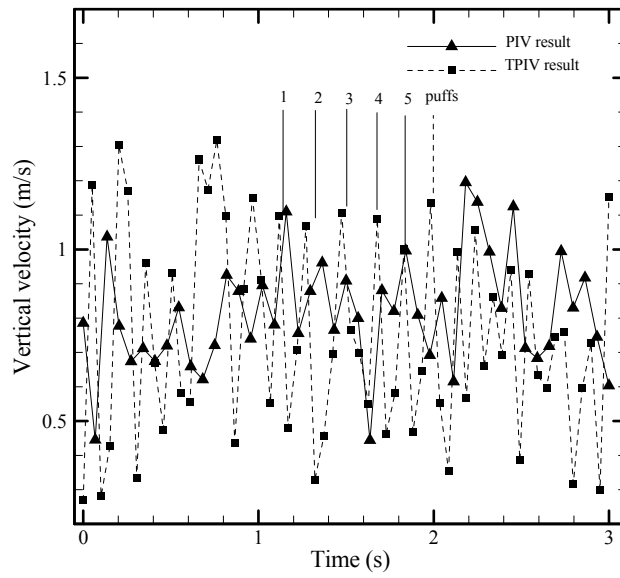


Fig. 7. Vertical velocity time histories obtained from PIV and TPIV algorithm.

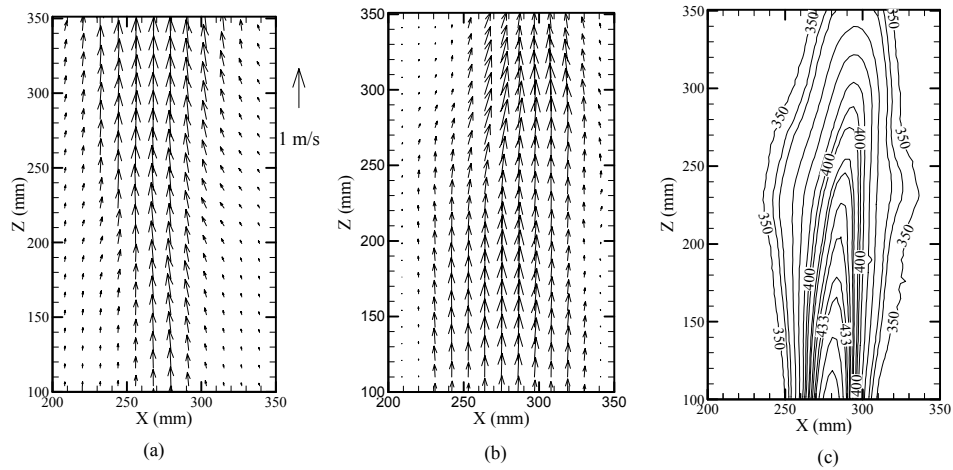


Fig. 8. Time-averaged velocity field obtained from PIV (a), TPIV algorithm (b), and corresponding time-averaged temperature field (c).

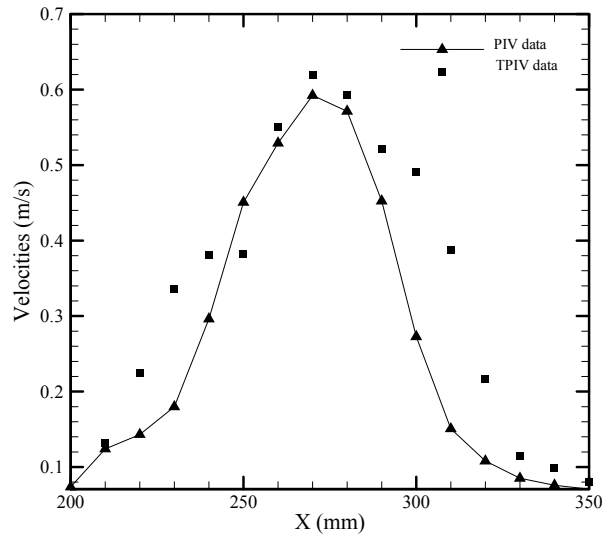


Fig. 9. Comparison of time-averaged vertical velocity profiles at $Z=200$ mm.

SUMMARY AND CONCLUSION

We investigated the velocity field in a fire plume by using a PIV technique and a TPIV algorithm. The TPIV algorithm uses instantaneous temperature fields captured by an IR camera to estimate corresponding instantaneous velocity fields. Velocity and temperature data are recorded at different framing rates, with different detectors and at different spatial locations. Time series data obtained from the same spatial location in each method was analyzed. By observing instantaneous velocity vector fields, comparing time series vertical velocity profiles and time-averaged velocity fields over 3 seconds from these two methods, we found that the velocities estimated by the TPIV algorithm appear reasonable, although the data appears a little bit lower than that measured by the PIV system. The possible reasons for this discrepancy were discussed. Further experimental investigation needs to be carried out to quantify the discrepancies. Overall TPIV algorithm provided us a relatively simple, inexpensive, and non-intrusive method to estimate velocities in a fire. It is expected that this method will prove useful in describing the temporal and spatial components of fire vortices that influence wildland fire spread.

ACKNOWLEDGEMENT

The funding source for this research is the USDA/USDI National Fire Plan administered through a Research Joint Venture Agreement No. 01-JV-11272166-135 with the Forest Fire Laboratory, Pacific Southwest Research Station, USDA Forest Service, Riverside, CA. The instrument names in this paper are provided for informational purposes only and do not constitute endorsement by the U.S. Department of Agriculture.

REFERENCES

- [1] Emmons, H.W., and Ying, S.J., "The Fire Whirl," *Eleventh Symposium (International) on Combustion*, 1967, pp. 475-486.

- [2] Byram, G.M., and Martin, R.E., "Modeling of Fire Whirlwinds," *Forest Science*, **16**, pp. 385-399, (1970).
- [3] Fendell, F.E., "Crown Streets," *Combustion Science and Technology*, **45**, pp. 311-315.
- [4] Haines, D.A., "Horizontal Roll Vortices and Crown Fires," *Journal of Applied Meteorology*, **21**, pp. 751-763, (1982).
- [5] McRae, D.J., and Flannigan, M.D., "Development of Large Vortices on Prescribed Fires," *Canadian Journal of Forest Research*, **20**, pp. 1878-1887, (1990).
- [6] Clark, T.L., Radke, L., Coen, J., and Middleton, D., "Analysis of Small-scale Convective Dynamics in a Crown Fire Using Infrared Video Camera Imagery," *Journal of Applied Meteorology*, **38**, pp. 1401-1420, (1999).
- [7] Raffel, M., Willert, C., and Kompenhans, J., *Particle Image Velocimetry*, Springer, Berlin Heidelberg, New York, 1998.
- [8] Reuss, D.L., Adrian, R.J., and Landreth, C.C., "Two-dimensional Velocity Measurements in a Laminar Flame Using Particle Image Velocimetry," *Combustion Science and Technology*, **67**, pp. 73-77, (1989).
- [9] Post, M.E., Goss, L.P., and Brainard, L.F., "Two-color Particle Imaging Velocimetry in a Diffusion Flame," *Spring Technical Meeting*, Central State Section of the Combustion Institute, 1991.
- [10] Driscoll, J.F., Sutkus, D.J., Roberts, W.L., Post, M.E., and Goss, L.P., "The Strain Exerted by a Vortex on a Flame Determined from Velocity Field Images," *31st Aerospace Sciences Meeting*, 1993, AIAA-93-0362.
- [11] Wolfrum, J., "Laser in Combustion: from Basic Theory to Practical Devices," *27th Symposium (International) on Combustion*, The combustion Institute, 1998, pp. 1-41.
- [12] Gray, C. *Optical Methods and Data Processing in Heat and Fluid Flow*, London, 1992, pp. 19-35.
- [13] Zhou, X.C., and Gore, J.P., "Study of Entrainment and Flow Patterns in Pool Fires Using Particle Imaging Velocimetry," National Institute of Standards and Technology Report GCR 97-706, 1996, 229 p.
- [14] Tieszen, R.S, O'hern, J.T., Schefer, W.R., Weckman, J.E., and Blanchat, K.T., "Experimental Study of the Flow Field In and Around A One Meter Diameter Methane Fire," *Combustion and Flame*, **129**, pp. 378-391, (2002).
- [15] Nezu, I., and Onitsuka, K., "Turbulent Structures in Partly Vegetated Open-channel Flows with LDV and PIV Measurements," *Journal of Hydraulic Research*, **39**, pp. 629-642, (2001).
- [16] Nezu, I., and Nakayama, T., "Space-time Correlation Structures of Horizontal Coherent Vortices in Compound Channel Flows by Using Particle-tracking Velocimetry," *Journal of Hydraulic Research*, **35**, pp. 191-208, (1997).
- [17] Riggan, P.J., Tissell, R.G., Lockwood, R.N., Brass, J.A., Pereira, A.P., Miranda, H.S., Miranda, A.C., Campos, T., and Higgins, R., "Remote Measurement of

- Energy and Carbon Flux from Wildfires in Brazil,” *Ecological Applications*, **14**, (3), pp. 855-872, (2004).
- [18] Riggan, P.J., Hoffmann, J.W., and J.A. Brass., “Estimating Fire Properties by Remote Sensing,” *2000 IEEE Aerospace Conference Proceedings*, 2000, **3**, pp. 173-179.
- [19] Riggan, P.J., Hoffman, J.W., “Field Applications of A Multi-spectral, Thermal Imaging Radiometer,” *1999 IEEE Aerospace Conference Proceedings*, 1999, **3**, pp. 443-449.
- [20] Riggan, P.J., Tissell, R.G., and Hoffman, J.W., “Application of the FireMapper Thermal-imaging Radiometer for Wildfire Suppression,” *2003 IEEE Aerospace Conference Proceedings*, 2003, **4**, pp. 1863-1872 .
- [21] Riggan, P.J., Hoffman, J.W., “FireMapper: A Thermal-imaging Radiometer for Wildfire Research and Operations,” *2003 IEEE Aerospace Conference*, 2003, **4**, pp.1843-1854.
- [22] Zhou, X., Sun, L., Weise, D.R., and Mahalingam, S., “Thermal Particle Image Velocity Estimation of Fire Plume Flow,” *Combustion Science and Technology*, **175**, pp. 1293-1316, (2003).
- [23] McCaffrey, B.J., and Heskestad, G., “A Robust Bidirectional Low-velocity Probe for Flame and Fire Application,” *Combustion and Flame*, **26**, pp. 125-127, (1976).
- [24] Cox, G., “Gas Velocity Measurement in Fires by the Cross-correlation of Random Thermal Fluctuations-a Comparison with Conventional Techniques,” *Combustion and Flame*, **28**, pp. 155-163, (1977).
- [25] Melling, A., “Tracer Particles and Seeding for Particle Image Velocimetry,” *Measurement Science and Technology*, **8**, pp. 1406-1416, (1997).
- [26] Glass, M., and Kennedy, I.M., “An Improved Seeding Method for High Temperature Laser Doppler Velocimetry,” *Combustion and Flame*, **29**, pp. 333-335, (1977).
- [27] Cetegon, B.M., and Ahmed, T., “Experiments on the Periodic Instability of Buoyant Plumes and Pool Fires,” *Combustion and Flame*, **93**, pp. 157-184, (1993).
- [28] Latham, D.A., “High Speed Photography of Fires,” *Second Symposium on Fire and Forest Meteorology*, American Meteorology Society, 1998, pp. 24-26, (Preprint Volume).